Naval Research Laboratory
Washington, DC 20375-5320

NRL/MR/5514--17-9692

# High Resolution Bathymetry Estimation Improvement with Single Image Super-Resolution Algorithm "Super-Resolution Forests"

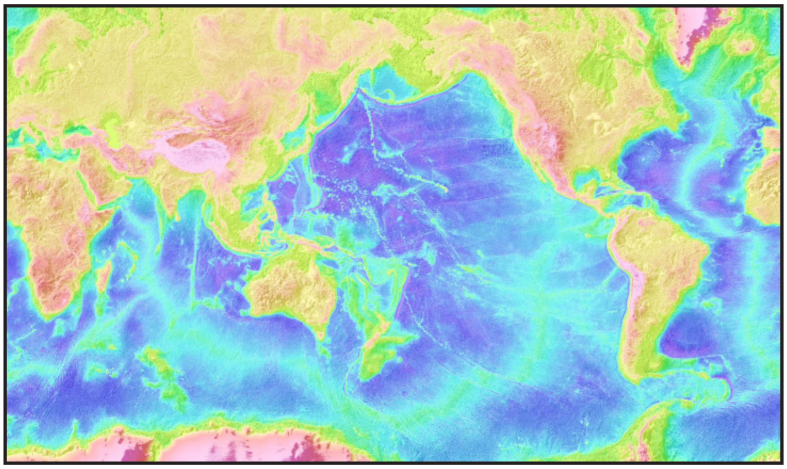

Dylan Einsidler

*Florida Atlantic University*
*Boca Raton, Florida*

Kristen Nock
Leslie Smith
David Bonanno

*Navy Center for Applied Research in Artificial Intelligence*
*Information Technology Division*

Paul Elmore
Warren Wood
Fred Petry

*Oceanography Division*
*Stennis Space Center, MS*

January 26, 2017

# REPORT DOCUMENTATION PAGE

*Form Approved*
*OMB No. 0704-0188*



**1. REPORT DATE** *(DD-MM-YYYY)*
26-01-2017

**2. REPORT TYPE**
Memorandum Report

**3. DATES COVERED** *(From - To)*

**4. TITLE AND SUBTITLE**

High Resolution Bathymetry Estimation Improvement with Single Image Super-Resolution Algorithm "Super-Resolution Forests"

**5a. CONTRACT NUMBER**

**5b. GRANT NUMBER**

**5c. PROGRAM ELEMENT NUMBER**

**6. AUTHOR(S)**

Dylan Einsidler,* Kristen Nock, Leslie Smith, David Bonanno, Paul Elmore, Warren Wood, and Fred Petry

**5d. PROJECT NUMBER**

**5e. TASK NUMBER**

**5f. WORK UNIT NUMBER**

**7. PERFORMING ORGANIZATION NAME(S) AND ADDRESS(ES)**

Naval Research Laboratory, Code 5514
4555 Overlook Avenue, SW
Washington, DC 20375-5320

**8. PERFORMING ORGANIZATION REPORT NUMBER**

NRL/MR/5514--17-9692

**9. SPONSORING / MONITORING AGENCY NAME(S) AND ADDRESS(ES)**

Naval Research Laboratory, Code 5514
4555 Overlook Avenue, SW
Washington, DC 20375-5320

**10. SPONSOR / MONITOR'S ACRONYM(S)**

**11. SPONSOR / MONITOR'S REPORT NUMBER(S)**

**12. DISTRIBUTION / AVAILABILITY STATEMENT**

Approved for public release; distribution is unlimited.

**13. SUPPLEMENTARY NOTES**

*Florida Atlantic University, 777 Glades Rd., Boca Raton, FL 33431

**14. ABSTRACT**

Using the single image super-resolution algorithm "Super-Resolution Forests (SRF)", this paper shows the ability to improve the prediction of high resolution bathymetry data. Borrowing the machine-learning technique of "training and testing" on a dictionary of sets data, we could create high resolution estimates of bathymetry data similar to estimates typically created with this technique using image data. By implementing a changed variance on the training process of the SRF algorithm, we were able to further increase the mean PSNR score of the high resolution estimated data from previously used bicubic interpolation.

**15. SUBJECT TERMS**

Bathymetry
Super-Resolution
Machine learning
Single image
Estimation

| 16. SECURITY CLASSIFICATION OF: a. REPORT | b. ABSTRACT | c. THIS PAGE | 17. LIMITATION OF ABSTRACT | 18. NUMBER OF PAGES | 19a. NAME OF RESPONSIBLE PERSON |
|---|---|---|---|---|---|
| Unclassified Unlimited | Unclassified Unlimited | Unclassified Unlimited | Unclassified Unlimited | 11 | Leslie N. Smith |
| | | | | | **19b. TELEPHONE NUMBER** *(include area code)* (202) 767-9532 |

**Standard Form 298 (Rev. 8-98)**
Prescribed by ANSI Std. Z39.18

# Table of Contents

## 1. Introduction

When it comes to understanding the bottom of the ocean, that is, the elevation of the seafloor around the globe, our current knowledge is very limited. In the public domain, 82% of the Earthós seafloor elevation (bathymetry) is only a prediction of depth (Weatherall et al., 2015). This prediction is derived from the inversion of satellite altimetry measurements of marine geoid height to seafloor topography (Smith and Sandwell, 1997; Calmant et al., 2002, Hu et al., 2015) (altimetry process shown in Figure 2). Sonar system surveys and regional grids provide knowledge of 18% Earthós bathymetry. These data constrain the inverse prediction for the remaining 82% of the globe.

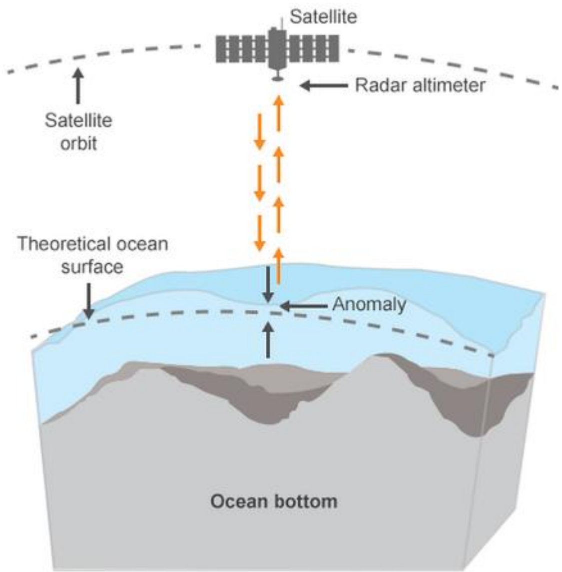


*Figure 2: How satellites predict bathymetry (Amos, J. (2014, October 2)*

The data collected from multibeam sonar systems is the highest quality data collected. Because the quality (resolution) of the data obtained from multibeam sonar systems is much greater than the data from satellites, we name the satellite data ñlow-resolutionò, and the sonar data ñhigh resolutionò. Ideally, all of our data would be high resolution. Instead, what the scientific community currently has is a mix of high and low-resolution data. The General Bathymetric Chats of the Oceans (GEBCO) uses both to grid the Earthós ocean floor at 30-arc second grid spacing (~ 1km). The latest grid is from 2014 (URL: http://www.gebco.net; Weatherall et al., 2015). In areas where only the predicted bathymetry (from altimetry) is available, the actual resolution of seafloor knowledge is ~ 10km. The 30-second grid adds more points to a smoothed surface using the Spline-In-Tension (Smith and Wessel, 1990).

## 2. Project Overview

For my summer internship project, I worked with a team to improve the U.S. Navyós knowledge of the planetós bathymetry. The team uses techniques borrowed from image processing called ñsingle image super-resolutionò to create new estimations of what the high-resolution data would look like if it were present instead of the low-resolution data.

The goal of this project was to apply a single-image super resolution technique to bathymetry data in a similar fashion, to estimate what the high resolution data might look like as if we collected the data from multibeam sonars. Creating high resolution estimations is useful for the Navy for a number of reasons. Mainly, it gives the Navyós maritime and submersible vehicles a better ability to navigate the seas. By creating the high resolution estimates, we are able to provide a better idea of what the ocean floor looks like. This can help navigate around dangerous situations such as protruding seamounts and deep/narrow ravines.

## 3. Single Image Super Resolution on Bathymetry Data

Single image super resolution is an image resolution improvement technique where if you have pairs of low resolution and high resolution images (of the same subject), you are able to use machine learning algorithms to ñlearnò or ñtrainò on those pairs

Manuscript approved August 19, 2016.

of images so that it can take only the low resolution image and yield a prediction of a high resolution image estimation. This is done by treating the pixels of the low resolution image as points of data, and mathematically interpolating those points to create an estimate of what the high resolution image would look like by referencing the already learned ñdictionaryò of image pairs. For example, if a high resolution image consists of 3600 pixels, and a low resolution image consists of 100 pixels (a difference of a scaling factor of 6), you can take the low resolution image and up-sample the pixels by interpolating them as data points to artificially create a high resolution estimation of 3600 pixels and then ñlearnò the difference (residuals) by using the comparison of pre-learned pairs of low resolution and high resolution images. An example of this estimation is shown in Figure 3.

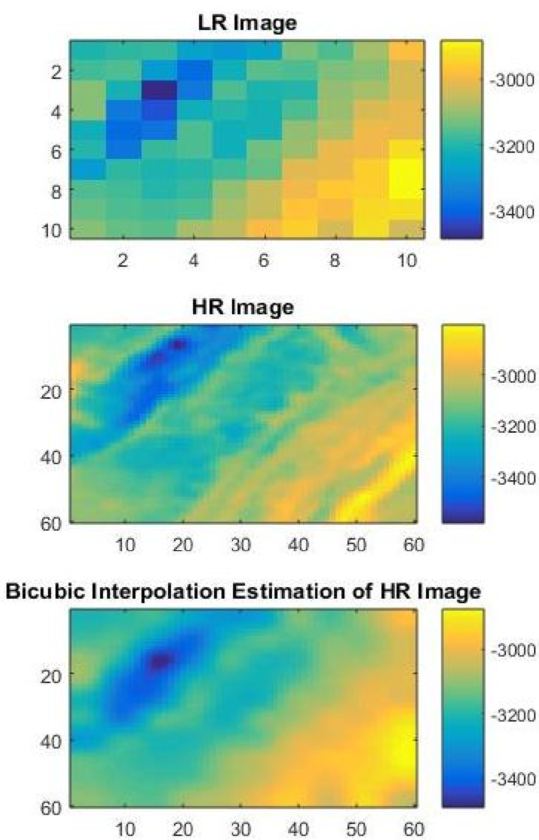


*Figure 3: Super-resolution using bicubic interpolation to produce an HR estimate using LR data (Images produced using Matlab).*

Before we could go about improving the Navyôs bathymetry data, we first had to confront some uncertainties. There were a number of things we were unsure of ï most of which stemmed from the fundamental differences between that nature of image data and bathymetry data. For instance, bathymetry data deals in elevation, whereas image data deals in variation of color/brightness (RGB value). This could introduce some problems regarding interpolation; specifically, how the data points in the z-direction (the height) would be treated. There are many different variations of the super-resolution technique, and one way in which they vary is in regards to the super-resolution method. For bathymetry data, we needed a super resolution technique that would preserve sharp changes - an interpolation method that would smooth out the data as little as possible. This is because the actual ocean floor is not very smooth ï there are sharp peaks and valleys, and in order to accurately represent the ocean floor with our high resolution data estimations, we must use a super-resolution technique that would smooth out these peaks and valleys as little as possible. Bicubic interpolation has the ability to produce high resolution estimations, however there is considerable a smoothing effect as a result. An example of this smoothing is shown in Figure 4.

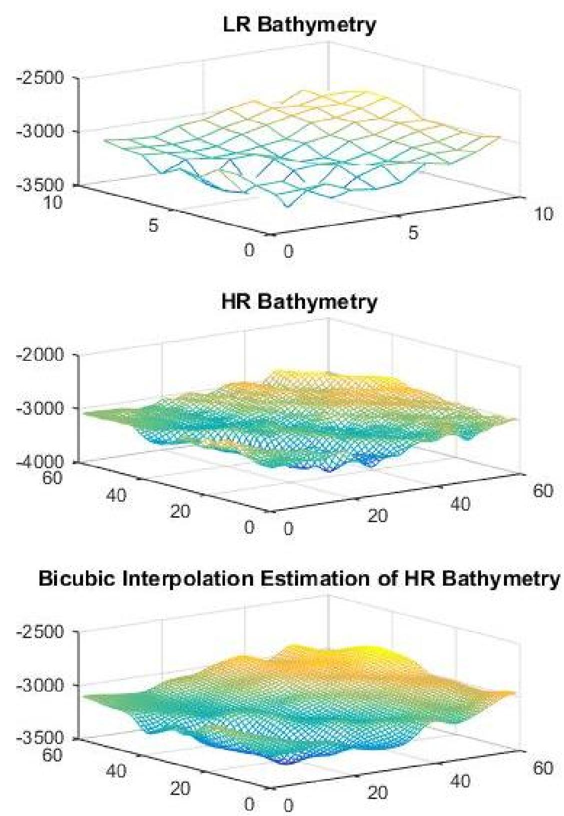


*Figure 4: Bicubic Interpolation shows the ability to predict HR bathymetry from LR data (similar to the capability of with image data), however there is considerable smoothing out of the prediction (Plots produced using Matlab).*

## 4. Super Resolution Forests

The super-resolution algorithm that was chosen to conduct our experiments on was called ñSuper-Resolution Forests (SRF)ò (Schulter, Leistner, and Bischof, (2015)). The code to run this algorithm was modified so that it would operate on bathymetry data instead of image data.

The SRF algorithm works as follows (see Figures 5 and 6): As input, you have pairs of low resolution and high resolution data. There are two main processes - training and testing. 80% of the input data is used for the training process, and the remaining 20% is reserved for the testing process. The size of the low resolution data is 10x10 points, and the size of the high resolution data is 60x60 points. The low resolution data is taken and undergoes bicubic interpolation, which is a common form of interpolation used on images. In doing so, it is up-sampled and has the same dimensions as the high resolution data. This new 60x60 interpolated data is labeled as the bicubic estimates. This estimated data is then compared to the original high resolution data and the SRF training process begins, resulting in a super-resolution forest (SRF) model which is created from the residuals of the original high resolution data and the up-sampled data.

Once the model is created, the testing process begins, and the reserved 20% of data pairs is used for testing. Each of the low resolution data blocks are up-sampled using bicubic interpolation. The super-resolution model is then applied to these bicubic estimates, yielding the final high resolution estimates. Each of the data blocks are tested with the remaining 20% percent of data pairs. After the forest is applied, the final high resolution estimates are created and are trimmed to have the dimensions of 48x48. This process of cropping the edges is a result of the fact that this SRF processing technique uses convolutional filters that cause distortions around the borders of an image. To compensate, the borders are removed, leaving us with 48x48 dimensions of undistorted data. The original high resolution data input is then trimmed to also have dimensions of 48x48 in order to match the high resolution estimates dimensions for comparison, and finally, a PSNR is computed and plotted for all data points.

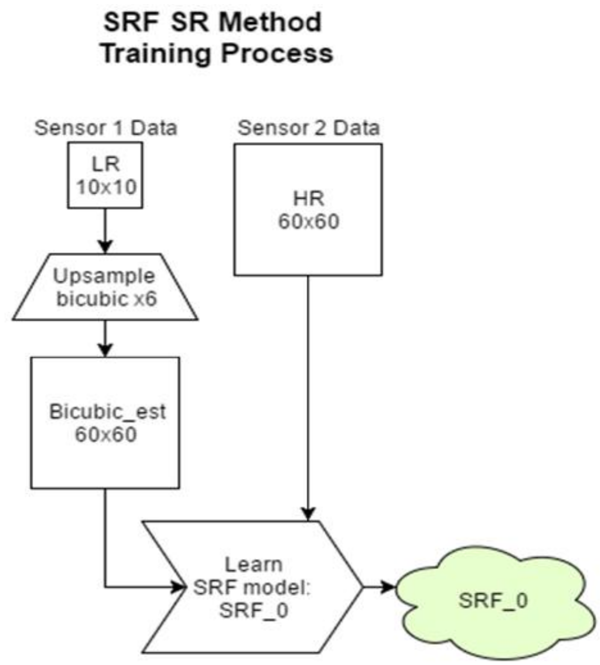


*Figure 5: Process 1/2 (Training) of the original SRF Algorithm*

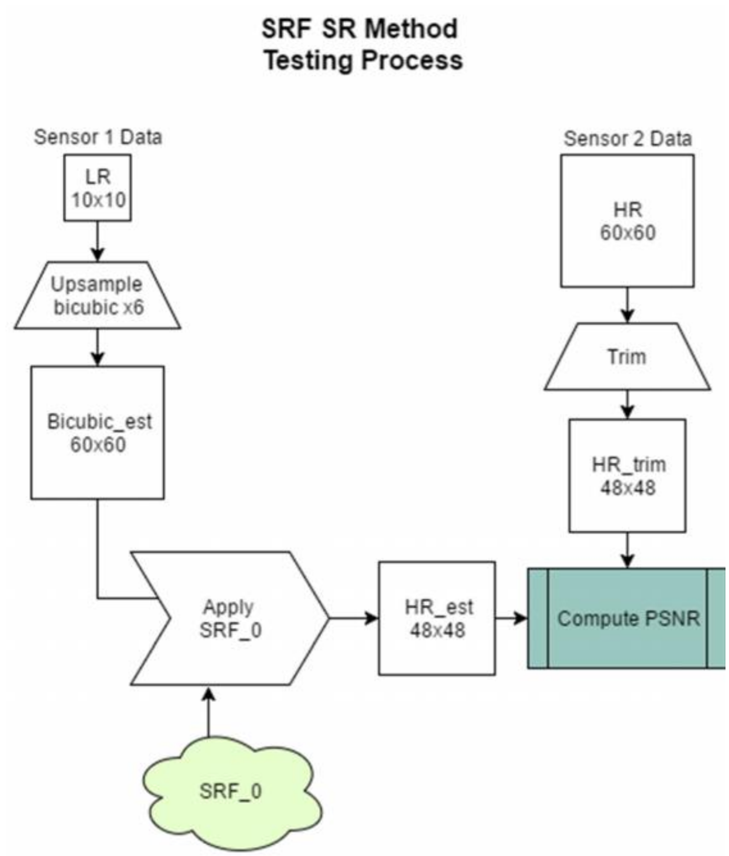


*Figure 6: Process 2/2 (Testing) of the original SRF Algorithm*

## 5. Changing the LR data variance

On the bathymetry data, the SRF process gave us a higher PSNR than bicubic interpolation (by about 1 dB).

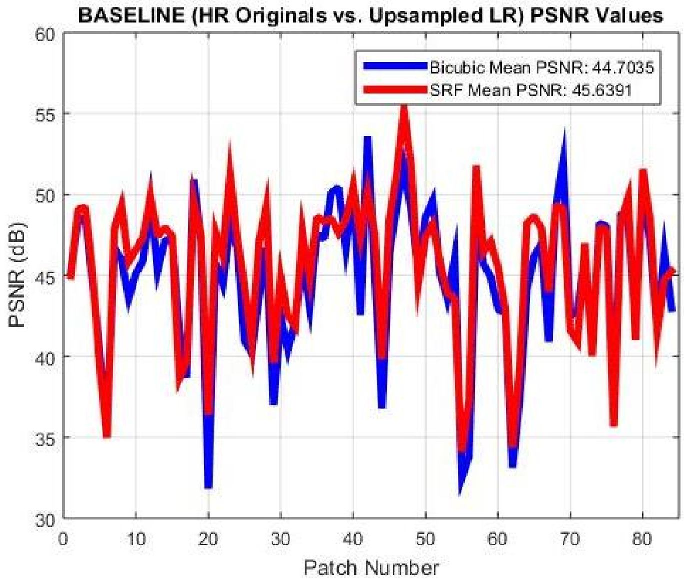


*Figure 7: PSNR comparison (with mean scores) between Bicubic Interpolation and SRF*

Figure 7 shows the comparison between the PSNR scores for all points of data having gone through both the bicubic interpolation and SRF algorithms. According to our results, the mean PSNR score from bicubic interpolation (44.7) was surpassed by the mean PSNR score from the SRF algorithm (45.6). Although it is a slight improvement, the team believed that we could do even better than a 1 dB increase for the SRF algorithm. Due to the smoothing nature of bicubic interpolation, there is a loss in detail of high frequency original bathymetry data while low frequency detail is preserved. This caused us to examine the variance of the data, and to do a comparison of before and after bicubic interpolation. If we could notice a relationship between the low resolution data and the high resolution data, then it could help us in estimating what high resolution bathymetry data would look like given only low resolution bathymetry data.

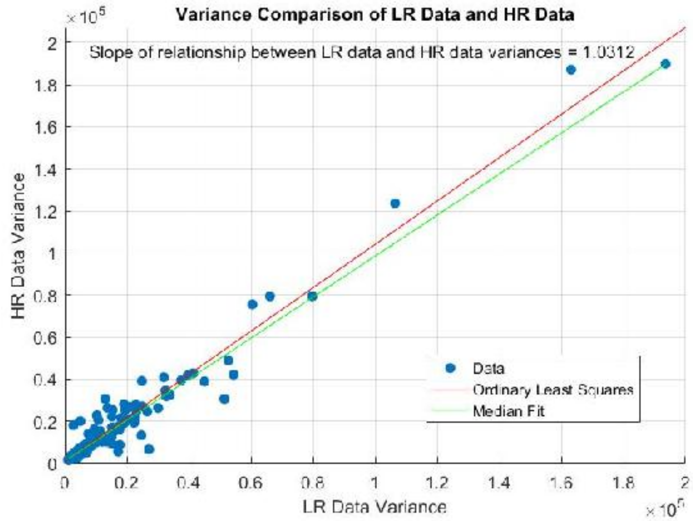


*Figure 8: Variance Comparison between LR and HR bathymetry data*

Figure 8 shows a comparison between the variance of the low resolution data against the variance of the high resolution data. The blue points represent variance values for each point of data, the red line represents an ordinary least squares line (a common way to plot a line of best fit), and the green line represents a median fit line (a line constructed by using the medians of each point between the two sets of data, respectively).We observed that there was a positive correlation between the variances (with a slope almost equal to 1). Having a correlation between the variances could enable us to predict estimations of high resolution data, given that we know both the low resolution data and the slope of what the correlation should be.

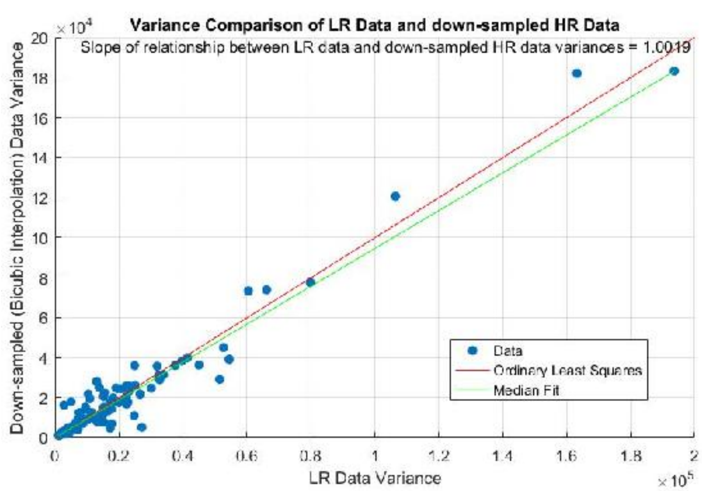


*Figure 9: Variance Comparison between LR and down-sampled HR (bicubic interpolation) bathymetry data*

We then took a look at the relationship between the variance of the low resolution data and the variance of the estimated low resolution data using bicubic interpolation to down-sample the known high resolution data (As shown in Figure 9).There were two main observations. Firstly, there was a drop in magnitude of the variance of the down-sampled data compared to the original high resolution data. Secondly, there was a slight decrease in slope-value. Knowing that the variance of the down-sampled data was decreasing and that there was a shift in slope (closer to 1), if we could move the data points away from the mean a certain distance *s* proportional to how far those data points are from the mean, then we could derive a simple expression to modify the variance of our estimated high resolution data to closer represent how it should appear in reality.

The mathematics behind this modified variance calculation is as follows:

The variance of the low resolution data (VarLR) is

$$VarLR = \frac{1}{N}\sum_{i}^{N}(x_i - \bar{x})^2$$

By modifying each point $x_i$ by a quantity $s(x - \bar{x})$, we can have the LR data variance (VarLR) be equal to the HR data variance (VarHR).

$$\begin{aligned} VarHR &= \frac{1}{N}\sum_{i}^{N}(x_i + s(x_i - \bar{x}) - \bar{x})^2 \\ &= \frac{1}{N}\sum_{i}^{N}(x_i + sx_i - \bar{s}\bar{x} - \bar{x})^2 \\ &= \frac{1}{N}\sum_{i}^{N}(x_i(1+s) - \bar{x}(1+s))^2 \\ &= \frac{1}{N}\sum_{i}^{N}(1+s)^2\,(x_i - \bar{x})^2 \\ &= (1+s)^2\frac{1}{N}\sum(x_i - \bar{x})^2 \end{aligned}$$

By substitution,

$$VarHR = (1+s)^2\,VarLR$$

And solving for s yields…

$$1 + s = \sqrt{\frac{VarHR}{VarLR}} \quad \rightarrow \quad \boxed{s = \sqrt{\frac{VarHR}{VarLR}} - 1}$$

By implementing an edited variance within certain locations of the SRF algorithm code, we could run experiments to see if implementing an edited variance could have any improvement on SRF's overall mean PSNR. Because bicubic interpolation is a step that occurs within the SRF algorithm, the drop in magnitude of variance after bicubic interpolation gave us reason to experiment with changing the variance before and after bicubic interpolation occurs within the algorithm.

## 6. The 7 trials

Within the SRF algorithm code, there were 3 locations at which the variance could be edited. The first location was before the bicubic estimates were created (before the SRF is learned and applied), the second location was after the bicubic estimates were created (also before the SRF is learned and applied), and the third location was after the high resolution estimates were created (after the SRF is learned and applied). Diagrams showing all 3 locations within the training and testing processes of the SRF algorithm are shown in Figures 11 and 12.

Since there were 3 locations where the variance could be edited, 7 trials could be conducted in total (the first 3 locations independently, first location in combination with the second location and then the third location, and finally all three locations simultaneously). A table showing which data would have its variance changed for each trial is displayed in Figure 10.

| | |
|---|---|
| Trial 1 | **1: Apply to LR [10x10] Data**<br>-before upsampling and before application of SRF |
| Trial 2 | **2: Apply to HR bicubic (interpolated) [60x60] Data**<br>-before application of SRF |
| Trial 3 | **3: Apply to HR estimated [48x48] Data**<br>-after application of SRF |
| Trial 4 | **4: Apply to LR and to HR bicubic (interpolated) Data** |
| Trial 5 | **5: Apply to LR and to HR estimated Data** |
| Trial 6 | **6: Apply to HR bicubic and to HR estimated Data** |
| Trial 7 | **7: Apply to LR, HR bicubic, and to HR estimated Data** |

*Figure 10: Table showing where the variance was changed along the SRF algorithm code for each trial, as well as what data is the input for each trial.*

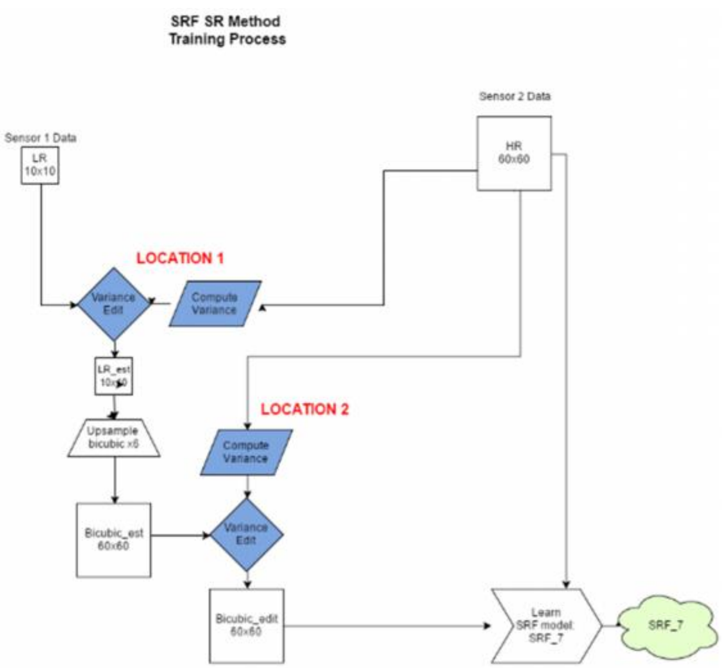


*Figure 11: Diagram showing the locations for the possible changes of variance in the SRF training process for all trials.*

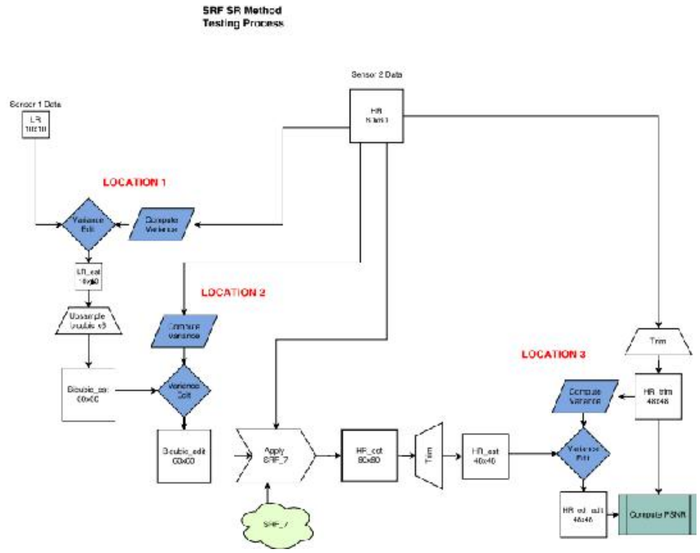


*Figure 12: Diagram showing the locations for the possible changes of variance in the SRF testing process for all trials.*

## 7. Results

Out of all of the 7 trials, the trial that yielded the greatest overall improvement from the mean PSNR score of the original SRF process was the PSNR score of trial 1 (as shown in Figure 13).

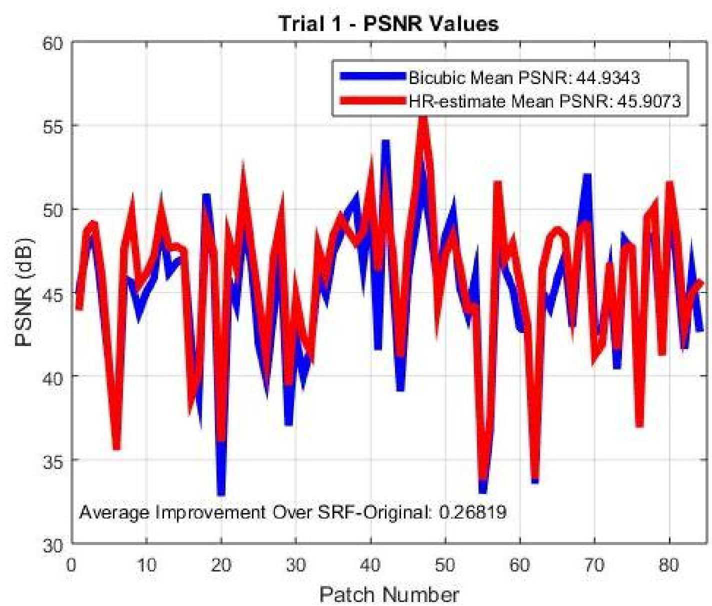


*Figure 13: PSNR comparison for Trial 1 (changing the variance of the low resolution data before it undergoes bicubic interpolation).*

This meant that implementing the edited variance before the bicubic estimates were created caused the mean PSNR to increase the most, and all combinations where either the variance was changed after the bicubic estimates were created or after the high resolution estimates were created caused the change in PSNR to be less than that of trial 1.

## 8. Discussion

As mentioned, for any case where the variance was changed after initial bicubic up-sampling, the change in mean PSNR was minimal. It is likely that the reason for this is that changing the variance after both the training and testing processes occur will introduce noise into the data, which will in turn cause the high resolution estimates to stray further away from the ground truth. Changing the variance early on in the SRF algorithm code (before bicubic interpolation occurs) would mean to edit the raw data as opposed to noisy data created later on along the code. Although trials 4, 5, and 7 also had the variance edit occur before the initial bicubic interpolation, because these trials had the variance of the data changed a second (or third) time later in the code after training/testing, it is suspected that the additional edits introduced noise into the data and thus worsened the improvement on the mean PSNR.

## 9. Conclusion and Future Remarks

These results show that it is possible to improve estimated high resolution bathymetry data with the use of a single image super-resolution technique, and the ability to further improve the estimations by altering the variance of the low resolution data as input in the training and testing processes of the SRF algorithm. A next step from here would be to investigate a way to estimate the desired variance of the data blocks without using "unknown" high resolution data. Another way to further improve the accuracy of high resolution data estimation would be to investigate how to adjust the variance spatially, instead of using one overall variance of the patch.

## References

[1] Calmant S, Berge-Nguyen M, and Cazenave A (2002), Global seafloor topography from a least-squares inversion of altimetry-based high-resolution mean sea surface and shipboard soundings, Geophysical Journal International, 151(3), 795-808. doi: 10.1046/j.1365-246X.2002.01802.x.

[2] Hu MZ, Li JC, Li H, Shen CY, Jin TY, and Xing LL (2015), Predicting global seafloor topography using multi-source data, Marine Geodesy, 38(2), 176-189. doi: 10.1080/01490419.2014.934415.

[3] Smith WHF, and Sandwell DT (1997). Global sea floor topography from satellite altimetry and ship depth soundings. Science, 277(5334), 1956–1962. Retrieved from <Go to ISI>://A1997XX84900033.

[4] Smith, WHF and Wessel P (1990). Gridding with continuous curvature splines in tension. Geophysics, 55(3), 293–305. doi:10.1190/1.1442837.

[5] Weatherall P., Marks KM, Jakobsson M., Schmitt T, Tani S, Arndt JE, Rovere M, Chayes D, Ferrini V, and Wigley R (2015). A new digital bathymetric model of the world's oceans. Earth and Space Science, 2(8), 331–345.

[6] Amos, J. (2014, October 2). Satellites detect 'thousands' of new ocean-bottom mountains. Retrieved July 21, 2016, from http://www.bbc.com/news/science-environment-29465446

[7] Schulter, Leistner, and Bischof (2015). Fast and Accurate Image Upscaling With Super-Resolution The IEEE Conference on Computer Vision and Pattern Recognition.

## List Of Figures